Chemisorption of Carbon Dioxide on Sodium Oxide Promoted Alumina

K. B. Lee, M. G. Beaver, H. S. Caram, and S. Sircar
Dept. of Chemical Engineering, Lehigh University, Bethlehem, PA 18015

DOI 10.1002/aic.11312
Published online September 19, 2007 in Wiley InterScience (www.interscience.wiley.com).

New equilibrium and column dynamic data for chemisorption of carbon dioxide from inert nitrogen at 250, 350, and 450°C were measured on a sample of sodium oxide promoted alumina, which was found to be a reversible chemisorbent for CO_2. The equilibrium chemisorption isotherms were Langmuirian in the low pressure region (p_{CO_2} <2.0 kPa) with a large gas–solid interaction parameter. The isotherms deviated from the Langmuirian behavior in the higher pressure region. A new analytical model which simultaneously accounted for Langmuirian chemisorption of CO_2 on the adsorbent surface and additional reaction between the gaseous and sorbed CO_2 molecules was used to describe the measured equilibrium data. The heats of CO_2 chemisorption and the additional surface reaction were, respectively, 64.9 and 37.5 kJ/mol. The column breakthrough curves for CO_2 sorption from inert N_2 on the chemisorbent as well as the desorption of CO_2 from the chemisorbent by N_2 purge at 350°C could be described by the linear driving force (LDF) model in conjunction with the new sorption isotherm. The same LDF mass transfer coefficients can be used to describe both sorption and desorption processes. The CO_2 mass transfer coefficients were (i) independent of feed gas CO_2 concentration in the range of the data at a given temperature, and (ii) a weak function of temperature. The ratio of the mass transfer zone length to the column length was very small due to highly favorable CO_2 sorption equilibrium. Several sequential cyclic CO_2 sorption–desorption column dynamic tests were conducted to demonstrate the apparent stability of the material. © 2007 American Institute of Chemical Engineers *AIChE J,* 53: 2824–2831, 2007

Keywords: chemisorption, carbon dioxide, sodium oxide promoted alumina, isotherm, chemisorption–surface reaction model, kinetics, desorption, cyclic stability

Introduction

Several new materials have been synthesized in the recent years which selectively and reversibly chemisorb CO_2 in the moderate temperature range of 200–600°C. Key examples include potassium carbonate promoted hydrotalcite,[1–5] sodium oxide promoted alumina,[6] and lithium zirconate.[7] The first two materials were originally developed by Air Products and Chemicals,[1–3,6] and they exhibit (i) nearly infinite selectivity of sorption for CO_2 from other gases such as CH_4, H_2, N_2, and steam at elevated temperatures, (ii) decent CO_2 sorption capacity, (iii) fast kinetics of CO_2 sorption, and (iv) completely reversible sorption of CO_2. The promoted hydrotalcite was used to develop a pressure swing sorption enhanced reaction (PSSER) scheme for direct production of a fuel-cell grade H_2 containing less than 30 ppm CO by steam reforming of methane (SMR) at a temperature of ~490°C without sacrificing the CH_4 to H_2 conversion.[1,8] The process was demonstrated in a pilot-scale unit.[8] Several conceptual variations of the original PSSER concept and their theoretical analysis were also published by various authors.[9–12] More recently, two different thermal swing sorption

Correspondence concerning this article should be addressed to S. Sircar at sircar@aol.com.

enhanced reaction (TSSER) schemes were proposed using the promoted hydrotalcite for (i) production of a fuel-cell grade H_2 by low-temperature SMR,[13,14] and (ii) simultaneous production of a fuel-cell grade H_2 and pure compressed CO_2 from synthesis gas.[15] The promoted alumina was used to develop a high-temperature pressure swing sorption scheme for removal of bulk CO_2 from a hot and wet waste gas at ~200°C and the process was demonstrated in a pilot-scale unit.[6]

The CO_2 chemisorption characteristics of different commercial and homemade samples of the K_2CO_3 promoted hydrotalcite sorbent have been published in the literature by various authors.[1–5,13–18] The most recent publication reports newly measured experimental data and their analysis on CO_2 sorption equilibria, kinetics, column dynamics, and heats on a commercial sample of the material at temperatures of 400 and 520°C in the pressure range of 0–304 kPa.[19] In contrast, there is no published data reporting the detailed chemisorption characteristics of CO_2 on the Na_2O promoted alumina. The purpose of the present work is to provide such data and their analysis using a commercial sample of the material donated to the Lehigh University by Air Products & Chemicals.

Experimental Apparatus and Procedure

A single-column adsorption apparatus was constructed to measure CO_2 sorption equilibria and CO_2 sorption breakthrough curves at temperatures of 250, 350, and 450°C on the Na_2O promoted alumina. Figure 1 is a schematic drawing of the apparatus. The key components included a sorption column (ID, D = 1.73 cm, length, L = 97.2 cm) which was surrounded by three different heating tapes with feed-back temperature controllers, gas heating and cooling exchangers, flow measuring devices (F), and switch valves (not shown). A layer of insulation was wrapped around the column over the heating tapes.

Several thermocouples were used to monitor the column temperature at three different heights (mid point, gas entrance, and exit ends). The system was also equipped with continuous CO_2 analyzers (a Pfeiffer quadrupole mass spectrometer and a GOW-MAC thermal conductivity analyzer).

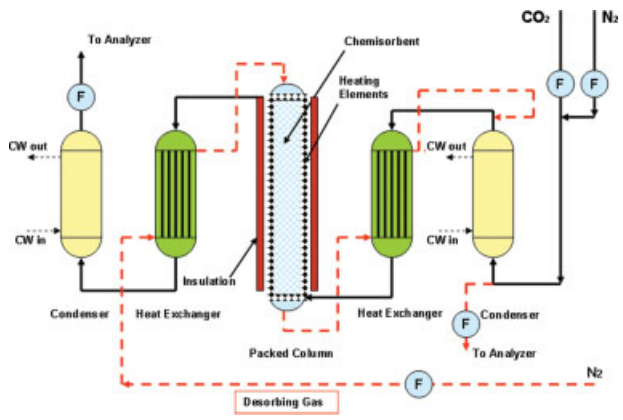

Figure 1. Schematic flow diagram of test apparatus.

[Color figure can be viewed in the online issue, which is available at www.interscience.wiley.com.]

The column was fully packed with the chemisorbent for measurement of CO_2 column dynamics. It was partially packed with the chemisorbent particles (packing length = 11 cm) in the gas exit end for measurement of CO_2 sorption isotherms. The rest of the column was packed with nonporous alumina particles in the second case. The packed column was externally heated to a constant temperature of T_0. The sorbent was then cleaned by flowing pure N_2, preheated to temperature T^*, at pressure P_0 until no impurity was detected in the effluent gas.

The adsorption experiment was carried out by flowing a CO_2 + N_2 (inert) gas mixture of known composition (mole fraction of CO_2 = y_0) through the precleaned column (filled with N_2 at P_0 and T_0) at pressure P_0. The feed gas mixture was preheated to T_0 in a heat exchanger. The feed gas inlet flow rate was constant (Q_0, mol/s) during the test. The CO_2 mole fraction $y(t)$ in the column effluent gas (CO_2 breakthrough profiles) was continuously monitored as a function of time (t) until the effluent gas CO_2 composition approached y_0 (time = t^0). The column effluent gas was cooled down to near ambient temperature in a heat exchanger and a portion of that gas was fed to the CO_2 analyzer. The column was equilibrated with CO_2 at partial pressure of p_0 (=P_0y_0) and temperature T_0 at the end of the adsorption test. The specific equilibrium amount of CO_2 chemisorbed (n^0, mol/kg) at a CO_2 partial pressure of p_0 and temperature T_0 could be calculated by the following mass balance equation (assuming that the gas phase is ideal):

$$n^0(p_0,T_0) = (Q_0/w)\left[t^0 y_0 - (1-y_0)\int_0^{t^0}\frac{y(t)}{[1-y(t)]}dt\right] - (\varepsilon p_0/\rho_s RT_0) \quad (1)$$

where ε is the helium void fraction of the column, ρ_s is the bulk density (g/mL) of the chemisorbent, w (g) is the amount of sorbent in the column, and R is the gas constant.

The column was then cleaned by flowing pure N_2 through the column and simultaneously heating the column to a higher temperature (T^*) in order to facilitate the desorption of CO_2. The inlet N_2 flow rate during regeneration was Q^* (mol/s). The effluent gas CO_2 composition [$y(t)$] was measured as a function of time (t) during the regeneration process. The specific amount of CO_2 removed from the column at time t [$N(t)$, mol/g] could be calculated by the following mass balance equation:

$$N(t) = [Q^*/w]\int_0^t \frac{y(t)}{[1-y(t)]}dt \quad (2)$$

The total amount of CO_2 removed from the column when the effluent gas CO_2 mole fraction approaches zero is N^0, which must be equal to the total specific amount of CO_2 in the column at the start of the desorption by purge experiment, if the chemisorption of CO_2 was completely reversible:

$$N^0 = [n^0 + \varepsilon p_0/\rho_s RT_0] \quad (3)$$

Table 1. CO_2 Chemisorption Isotherms on Na_2O Promoted Alumina

	n_{CO_2} (mol/kg)								
	T = 250°C			T= 350°C			T = 450°C		
p_{CO_2} (atm)*	Expt.	Model	Error** (%)	Expt.	Model	Error** (%)	Expt.	Model	Error** (%)
0	0		0	0	0		0	0	
0.005	0.217	0.215	+0.9	0.090, 0.096	0.057	+63.2			
0.01	0.243	0.249	−2.4	0.117	0.096	+21.9			
0.02	0.273	0.272	+0.4	0.150	0.146	+2.7			
0.05	0.360	0.296	+21.6	0.146	0.214	−31.8			
0.1	0.431	0.333	+29.4	0.198, 0.260	0.262	−12.6	0.172	0.142	+21.1
0.2	0.412, 0.474	0.435	+1.8	0.273	0.323	−15.5			
0.3	0.541, 0.656	0.540	+10.8	0.396	0.377	+5.0	0.200	0.253	−20.9
0.4	0.481, 0.584	0.625	−14.8						
0.5	0.473, 0.643	0.687	−18.8	0.512	0.474	+8.0	0.290	0.325	−10.8
0.6	0.727	0.732	−0.7						
0.7	0.765	0.765	0.0	0.546	0.549	−0.5			
0.8	0.685, 0.712, 0.727, 0.781, 0.839	0.788	−4.9	0.576	0.578	−0.3	0.490, 0.554	0.407	+28.3
0.9	0.778	0.806	−3.5						
1.0				0.582	0.625	−6.9			
2.0	0.911	0.867	+5.1	0.726	0.729	−0.4	0.659	0.582	+13.2
3.0	1.013	0.877	+15.5	0.760	0.760	0.0	0.696	0.640	+8.7
Average error (%)			8.7%			12.9%			17.2%

*1 atm = 101.3 kPa.
** Error = $[\{n_{expt} - n_{model}\}/n_{model}] \times 100$.

The adsorption and desorption experiments could be repeated using different values of p_0 at any given temperature (T_0) in order to generate the entire CO_2 chemisorption isotherm, $[n^*(p_0,T_0)]$, at T_0.

The bulk and particle densities of the chemisorbent were measured by us to be 0.694 and 2.222 g/mL, respectively. The total void fraction of the column was measured to be 0.701. The diameter (d_p) of the spherical chemisorbent particles was ~0.35 cm. The adsorbed CO_2 was completely desorbed by N_2 purge when the desorption process was facilitated by externally heating the column to 350–450°C (T^*). The test results are summarized in the following sections. Only those data points where the amounts of CO_2 adsorbed and desorbed matched within ±10–15% during the ad(de)sorption experiments are reported, thereby guaranteeing reversible chemisorption.

CO_2 Chemisorption Isotherms on Na_2O Promoted Alumina at 250, 350, and 450°C

Table 1 reports the experimentally measured chemisorption equilibrium data points at three temperatures. The multiple values of CO_2 chemisorption capacities at any given CO_2 partial pressure in the table indicate the extent of data reproducibility. It may be seen that the maximum scatter in the measured equilibrium amount of CO_2 chemisorption at any given partial pressure of CO_2 and temperature T is less than ±15% of the average value at that condition. Figure 2 shows the experimentally measured chemisorption isotherms of CO_2.

The measured equilibrium isotherm data could not be described by the classical Langmuir model for chemisorption of gases as shown by Figure 3 where the quantity $[p_{CO_2}/n_{CO_2}]$ is plotted against p_{CO_2} for the 250°C data. The plot should yield a straight line if the Langmuir model is obeyed. The low pressure data points of the isotherm ($p_{CO_2} < 2.0$ kPa) were used to establish the region of Langmuir model fit in Figure 3 so that the Henry's Law constant for the isotherm could be accurately determined. This is very important because the correct knowledge of the Henry's Law constant for the CO_2 chemisorption isotherm is critical for reliable estimation of CO_2 desorption characteristics from the chemisorbent (Figure 7).[20] Figure 3 shows that the measured isotherm significantly deviates from the Langmuir model in the high pressure region.

A similar behavior was observed for chemisorption of CO_2 on K_2CO_3 promoted hydrotalcite in the temperature range of 400–520°C and a novel simultaneous chemisorption and surface reaction model was proposed to describe the equilibrium isotherms.[19] The essential features of the model are summarized in the next section.

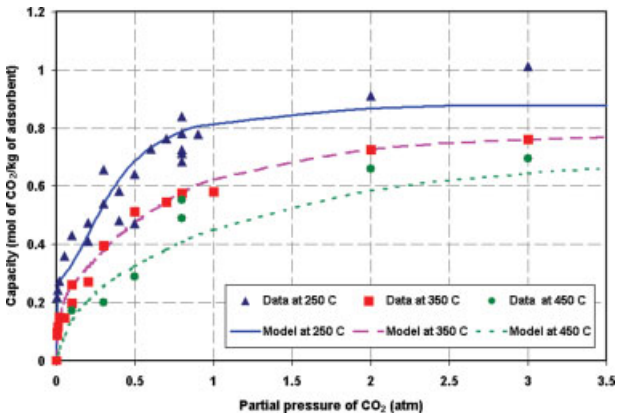

Figure 2. CO_2 chemisorption isotherms on Na_2O promoted alumina.

[Color figure can be viewed in the online issue, which is available at www.interscience.wiley.com.]

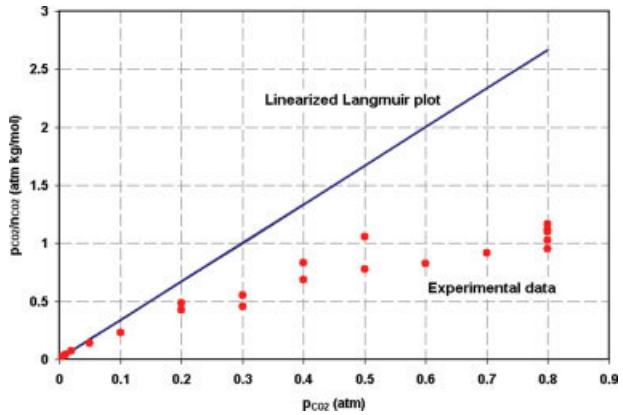

Figure 3. Linearized Langmuir plot of the CO_2 chemisorption isotherm at 250°C.

[Color figure can be viewed in the online issue, which is available at www.interscience.wiley.com.]

New chemisorption–surface reaction model

It was assumed that two simultaneous reactions are occurring when a gas A is contacted with the chemisorbent:

- Reversible chemisorption of A on the surface of the chemisorbent:

$$\text{A (gas)} + \text{S (empty site)} \leftrightarrow \text{A—S (chemisorbed A)} \quad (4)$$

- Reversible chemical complexing between the gas and the chemisorbed molecules of A:

$$a\text{A (gas)} + \text{A} - \text{S} \leftrightarrow \text{A}_{(a+1)}\text{—S (surface complex)} \quad (5)$$

Equation 4 describes the classic Langmuirian mechanism of chemisorption where one molecule of gas A is chemisorbed on one empty chemisorption site of an energetically homogeneous sorbent.[21] The components S and A–S, respectively, represent the empty site and the chemisorbed A molecule. Equation 5 describes the additional complexation reaction between the gas molecules of component A and the chemisorbed A molecules. It is assumed that a molecules of gas A react with each chemisorbed A molecule to form one molecule of the surface complex $A_{(a+1)}$–S.

The analytical equation for describing the equilibrium chemisorption isotherm by the proposed model is given by[19]:

$$n^*(P,T) = \frac{mK_CP[1 + (a+1)K_RP^a]}{[1 + K_CP + K_CK_RP^{(a+1)}]} \quad (6)$$

where n^* is the specific equilibrium amount (mol/kg) of gas A sorbed on the chemisorbent at pressure P (atm) and temperature T (K). The parameters of Eq. 6 are m (mol/kg), the saturation chemisorption capacity of the chemisorbent surface; K_C (atm^{-1}), the equilibrium constant for the chemisorption reaction; K_R (atm^{-a}), the equilibrium constant for the additional complexation reaction; and a, the stoichiometric coefficient for the complexation reaction. The thermodynamic constants (K_C and K_R) are exponential functions of temperature:

$$\frac{d\ln K_C}{dT} = -\frac{q_C}{RT^2}; \quad \frac{d\ln K_R}{dT} = -\frac{\Delta H_R}{RT^2} \quad (7)$$

$$K_c = K_c^0 \exp[q_C/RT]; \quad K_R = K_R^0 \exp[\Delta H_R/RT] \quad (8)$$

where q_C and ΔH_R (kJ/mol) are, respectively, the molar isosteric heat of chemisorption and the heat of additional surface reaction. K_C^0 (atm^{-1}) and K_R^0 (atm^{-a}) are constants.

It can be shown that (i) Eq. 6 has the same form as the Langmuir isotherm model (Eq. 9)[21] in the low pressure region, and (ii) n^* asymptotically approaches a saturation capacity [$n^m = m(a + 1)$] at the limit of $P \to \infty$:

$$n^*(P,T) = \frac{mK_CP}{[1 + K_CP]} \quad \text{for small values of } P \text{ or } n^* \quad (9)$$

The solid and dashed lines of Figure 2 show the fit of the experimental chemisorption isotherms of CO_2 on Na_2O promoted alumina at 250, 350, and 450°C by Eq. 6. The model parameters are given in Table 2.

It may be seen from Figure 2 that the new model describes the experimental chemisorption isotherm data fairly well. Table 1 gives the CO_2 chemisorption capacities estimated by the model equation for each experimental data condition. The average differences between the experimental and the calculated CO_2 capacities are, respectively, 8.7%, 12.9%, and 17.2% for isotherms at 250, 350, and 450°C. These differences are comparable with the experimental errors for the data. The heats of chemisorption and the surface reaction were estimated to be, respectively, 64.9 and 37.5 kJ/mol.

The corresponding preexponential constants (Eq. 8) were, respectively, 0.000164 (K_C^0, atm^{-1}) and 0.001417 (K_R^0, atm^{-a}). It may be seen from Table 2 that the parameter a was also an exponential function of temperature:

$$a = 0.72644 \exp\left[\frac{4.39(\text{kJ/mol})}{RT}\right] \quad (10)$$

The last column of Table 2 gives the Henry's law constants [$K_H = mK_C$, mol/(kg atm)] for the chemisorption isotherms at different temperatures. The CO_2 isotherm at 250°C is rather steep in the Henry's law region but the heat of chemisorption is very moderate.

The simultaneous chemisorption and surface reaction model introduces an inflection in the isotherm shape in the low pressure region of the isotherm where the Langmuirian monolayer for chemisorption of CO_2 is nearly completed. This is most pronounced for the CO_2 isotherm at 250°C as shown by Figure 2. The inflection cannot be caused by phase transition and subsequent hysteresis as encountered in physisorption of condensable vapors in mesoporous solids because the system temperatures in the present case (>523.1 K) are

Table 2. Parameters of Chemisorption-Surface Reaction Model for Sorption of CO_2 on Na_2O Promoted Alumina

T (°C)	m (mol/kg)	a	K_C (atm^{-1})	K_R (atm^{-a})	$K_H = mK_C$ (mol/kg/atm)
250	0.295	2.0	536	8	158
350	0.295	1.7	48.3	2	14.2
450	0.295	1.5	8.47	0.73	2.45

Table 3. Comparative Chemisorption of CO_2 on Two Materials

Chemisorbent	m (mol/kg)	a	q_C (kJ/mol)	ΔH_R (kJ/mol)	K_H (mol/kg/atm)
K_2CO_3 promoted hydrotalcite at 400°C	0.250	2.5	21.0	42.2	9.35
Na_2O promoted alumina at 350°C	0.295	1.7	64.9	37.5	14.2

significantly higher than the critical temperature of CO_2 (304.1 K) and condensation of CO_2 in the sorbent pores is not feasible. Furthermore, the heat of surface complexation reaction which causes the inflection in the isotherm shape is estimated to be ~37.5 kJ/mol of CO_2 which is much larger than the heat of condensation of CO_2 (~25.1 kJ/mol).

Table 3 compares the equilibrium characteristics for chemisorption of CO_2 on K_2CO_3 promoted hydrotalcite at 400°C[19] and Na_2O promoted alumina at 350°C and Figure 4 compares the corresponding sorption isotherms. Table 3 and Figure 4 clearly show that the Na_2O promoted alumina provides a much higher CO_2 sorption capacity at 350°C in the low pressure region than the K_2CO_3 promoted hydrotalcite at 400°C. The Henry's law constant for CO_2 chemisorption on the promoted alumina at 350°C is ~50% larger than that on promoted hydrotalcite at 400°C. On the other hand, the CO_2 sorption capacities of the promoted hydrotalcite are ~15% higher than those of the promoted alumina in the high pressure region.

The heat of CO_2 chemisorption on the promoted alumina is ~3 times larger than that on the promoted hydrotalcite. Thus there will be a larger temperature coefficient of working CO_2 sorption capacity on the promoted alumina by a thermal swing sorption process. On the other hand, desorption of CO_2 from the material will be more difficult. Nevertheless, the heats on the alumina are moderate (less than the heat of physisorption of H_2O on zeolites, ~75.3 kJ/mol) making it an attractive practical chemisorbent for a TSSER process for selective removal of CO_2. Interestingly, the heats of additional complexation reaction for both materials are comparable.

These properties suggest that the promoted alumina may be a suitable candidate for removal of dilute (>5%) or bulk CO_2 from a hot (150–350°C) and wet waste gas without precooling and predrying as has been done earlier,[6] as well as for design of a SER processes for production of fuel-cell grade H_2 using an admixture of the chemisorbent and a catalyst as already proposed.[13–15]

It should also be mentioned here that several articles have been published which promoted the use of CaO or dolomite as a reversible CO_2 chemisorbent for use in SER concepts for production of H_2 by SMR. A review of these works and the merits and demerits of CaO as the chemisorbent can be found elsewhere.[1,13]

CO_2 Sorption Column Dynamics on Promoted Alumina

CO_2 breakthrough experiments were carried out at 250 and 350°C using the column apparatus (97.2-cm long). The chemisorbent was cleaned by N_2 purge before each run. Different compositions of $CO_2 + N_2$ mixtures were used as the feed gas. The feed gas and the column pressures for all runs were near ambient. The feed gas was preheated to 250 or 350°C and its flow rate was ~250 mL/min. The response time of the GOW-MAC CO_2 analyzer was measured by directly flowing $CO_2 + N_2$ gas mixtures of different compositions through the analyzer and recording the time delay in output CO_2 compositions. The column sorption breakthrough data were then corrected to account for the analyzer response time delay. Figure 5 shows two examples of CO_2 breakthrough profiles for feed CO_2 compositions (y_0) of 40 and 60 mol % at 250°C. Figure 6 shows two similar examples of CO_2 breakthrough profiles at 350°C. The plots are normalized CO_2 mole fractions [$y(t)/y_0$] in the column effluent gas as a function of normalized time [t/t^*], where t^* is the isothermal breakthrough time under local equilibrium condition. t^* could be calculated by:

$$Q_0 y_0 t^* = w[n^0 + (\varepsilon p_0/\rho_s R T_0)] \tag{11}$$

Figures 5 and 6 show that the CO_2 mass transfer zones are nearly vertical. This indicates very efficient utilization of the column capacity. The column inefficiency was estimated by the LUB (length of the unused bed) concept[22]:

$$\frac{\text{LUB}}{L} = \left[1 - \frac{t^b}{t^*}\right] \tag{12}$$

where t^b is the time of incipient breakthrough of CO_2 from the column of length L.

The LUB is equal to zero under local equilibrium conditions (100% of the column adsorption capacity for the adsorbate is utilized). The existence of a mass transfer resistance for adsorption causes the LUB to be finite, and thus, the ratio (LUB/L) is a qualitative measure of column inefficiency. The (LUB/L) ratios for the data of Figures 5 and 6

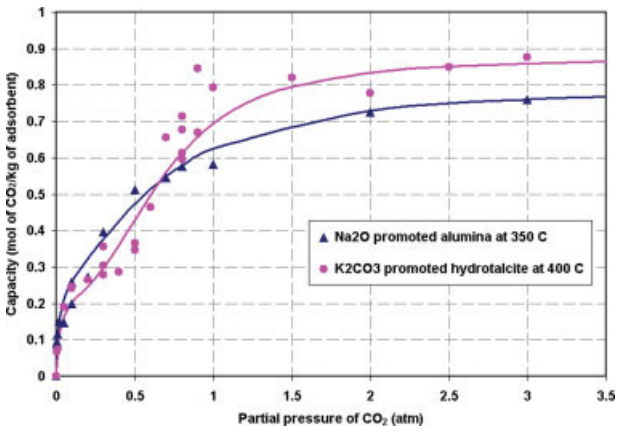

Figure 4. Comparative chemisorption isotherms of CO_2 on two materials.

[Color figure can be viewed in the online issue, which is available at www.interscience.wiley.com.]

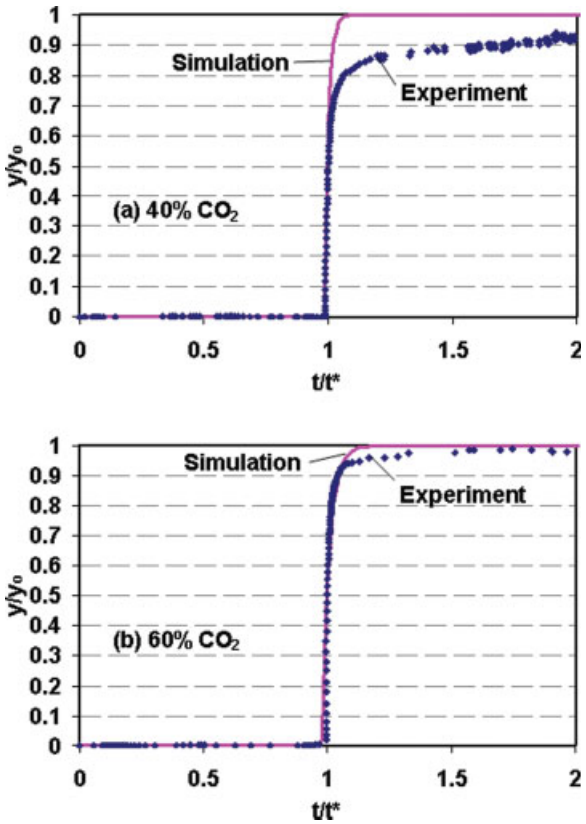

Figure 5. CO_2 column breakthrough data on promoted alumina at 250°C.

[Color figure can be viewed in the online issue, which is available at www.interscience.wiley.com.]

were calculated (t^b corresponding to $y/y_0 = 0.01$) to be less than 5.0% indicating very high utilization of the column CO_2 capacity.

CSTR in series model for analysis of breakthrough data

A conventional "continuous stirred tank reactors (CSTRs) in series" model[13,19,23] was adapted for quantitative estimation of the CO_2 mass transfer coefficients on the Na_2O promoted alumina sample from the column breakthrough data shown in Figures 5 and 6. The ordinary differential equations of the model were solved using Matlab function ODE15s. A fairly large number of tanks in series (500) were used to simulate the sharp mass transfer zones for chemisorption of CO_2. No further changes in the solutions of the equations were observed when the number of tanks in series exceeded 500. The model could be used to simulate isobaric, adiabatic, or isothermal sorption of CO_2 in a packed column of the chemisorbent using the sorption equilibria of Eq. 6 and the linear driving force (LDF) mass transfer mechanism for CO_2 sorption[24]:

$$\text{LDF model:} \quad \frac{dn(t)}{dt} = k[n^*(t) - n(t)] \tag{13}$$

Equation 13 gives the local rate of ad(de)sorption of CO_2 from an inert gas inside the column. $n(t)$ is the specific amount (mol/kg) of CO_2 chemisorbed at time t and $n^*(t)$ is the specific equilibrium adsorption capacity of CO_2 at the prevailing gas phase at pressure P_0, temperature $T(t)$ and CO_2 mole fraction of $y(t)$. n^* is given by Eq. 6 for a given set of P_0, y, and T. The parameter k (time^{-1}) is the LDF mass transfer coefficient for CO_2 sorption.

The key assumptions in the dynamic simulation model include (i) ideal gas behavior, (ii) instantaneous thermal equilibrium between the gas and the solid inside the column, (iii) absence of axial dispersion, (iv) absence of column pressure drop, (v) constancy of k value, and (vi) perfectly isothermal or adiabatic column behavior.

The simulated isothermal CO_2 breakthrough profiles are shown in Figures 5 and 6. They trace the experimental data nearly quantitatively for most of the time [between (y/y_0) values of 0 to ~0.8]. The lack of fit in the latter part of the breakthrough curve is very likely due to the column nonisothermality (±2% of base temperature) as explained earlier.[19,25] The same values of the CO_2 mass transfer coefficients (k = 4.0 min^{-1} at 250°C and 5.0 min^{-1} at 350°C) were used to fit both sets of breakthrough data at any given temperature. This demonstrated that k was independent of feed gas CO_2 concentration in the range of the data. Furthermore, there was ~25% increase in the overall CO_2 mass transfer coefficient when the system temperature was increased from 250 to 350°C. The small LUB/L for this system was caused by highly favorable chemisorption isotherm

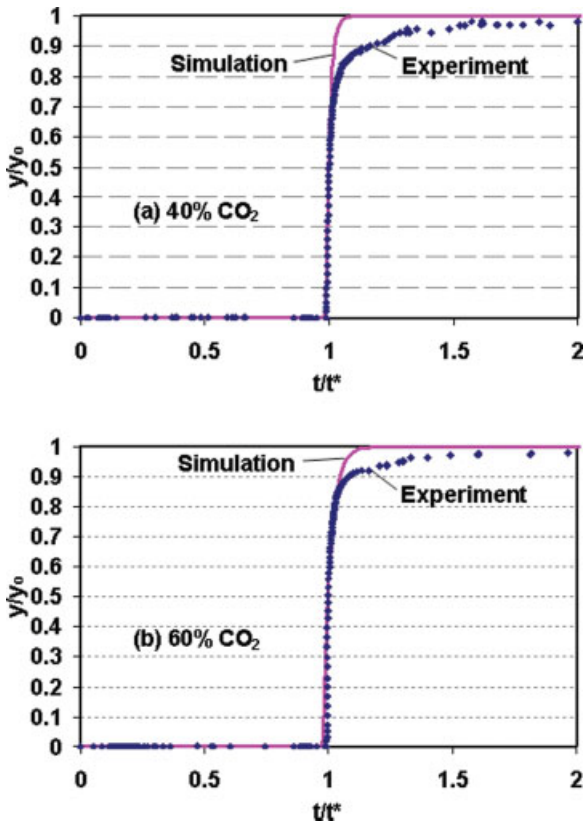

Figure 6. CO_2 column breakthrough data on promoted alumina at 350°C.

[Color figure can be viewed in the online issue, which is available at www.interscience.wiley.com.]

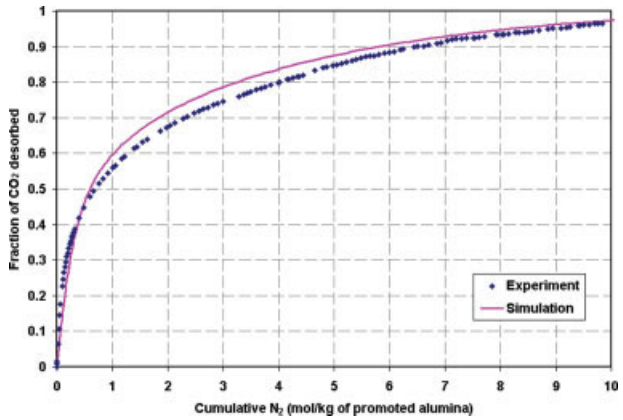

Figure 7. CO_2 desorption characteristic from Na_2O promoted alumina at 350°C.

[Color figure can be viewed in the online issue, which is available at www.interscience.wiley.com.]

of CO_2 which increases the driving force for sorption (Eq. 13) and favors shelf-sharpening of the zone despite a moderate value of the mass transfer coefficient.

CO_2 Desorption from Promoted Alumina

Experiments were conducted to evaluate the reversible desorption of CO_2 from the Na_2O promoted alumina. The packed column (97.2-cm long) was saturated with a gas stream containing 40% CO_2 in N_2 at a temperature of 350°C and a total pressure of 101.3 kPa. The saturated column was then purged with pure N_2 at 350°C and ambient pressure. The feed gas flow rate was 250 mL/min and the purge gas flow rate was 400 mL/min. The effluent gas flow rate and its composition were measured as functions of time. The effluent profile was integrated to calculate the fraction of CO_2 desorbed by purge as a function of the specific cumulative amount of N_2 purge gas used. Figure 7 shows an example of the desorption characteristic of CO_2.

The solid line of Figure 7 is the simulated desorption profile of CO_2 from the promoted alumina at 350°C using the CSTR model in conjunction with the equilibrium isotherm of Eq. 6 and the LDF model for CO_2 mass transfer ($k = 5.0$ min^{-1}). The conditions of simulation were identical with those of the test. It may be seen that the calculated desorption characteristics closely follow those of the test. This indicates that the kinetics of desorption of CO_2 can also be described by the LDF model using the same value of the mass transfer coefficient as that for sorption.

Cyclic Stability of Promoted Alumina

A preliminary evaluation of the cyclic stability of Na_2O promoted alumina for repeated chemisorption–desorption of CO_2 was carried out by packing a section of the column apparatus (11-cm length) with the sorbent and (i) equilibrating the section with 80% CO_2 in N_2 at ambient pressure and 250°C, followed by (ii) complete desorption of CO_2 using N_2 purge at ambient pressure and 350°C. The process was repeated for nine cycles. The amount of CO_2 sorbed at 250°C and a partial pressure of 81.1 kPa was estimated by analysis of the breakthrough data in each cycle. Figure 8 summarizes the results. It may be seen that the CO_2 sorption capacity initially decreased somewhat and then became practically stable (within experimental error) after the third cycle. These data are an evidence of cyclic stability of the chemisorbent under the test conditions for a thermal swing operation.

Summary

A column dynamic test apparatus was used to measure (i) new equilibrium data for reversible chemisorption of CO_2 on Na_2O promoted alumina at 250, 350, and 450°C in the CO_2 partial pressure range of 0–3 atm (304.0 kPa), and (ii) CO_2 column breakthrough dynamics for sorption of bulk CO_2 from mixtures with inert N_2 at 250 and 350°C and a total gas pressure of 1 atm (101.3 kPa). The isotherm for chemisorption of CO_2 could be described by the Langmuir model in the low CO_2 partial pressure region but the isotherm deviated significantly from the Langmuir model at higher CO_2 partial pressures. A new analytical equilibrium model based on simultaneous chemisorption of CO_2 on the sorbent and additional reaction of gaseous CO_2 with chemisorbed CO_2 was used to describe the measured isotherm data. The heats of chemisorption of CO_2 and the additional surface reaction were, respectively, 64.9 and 37.5 kJ/mol.

The CO_2 column breakthrough curves could be adequately described using the LDF model and the new chemisorption isotherm. A CSTR in series model was used to extract the LDF mass transfer coefficient ($k \sim 4.0$ and 5.0 min^{-1} at 250 and 350°C, respectively) from the breakthrough data. The mass transfer coefficient was found to be independent of CO_2 loading and a weak function of temperature in the range of the reported data. The desorption of CO_2 from a column packed with promoted alumina by N_2 purge can also be adequately described using the LDF model and using the same CO_2 mass transfer coefficients as for sorption.

Preliminary cyclic tests consisting of CO_2 chemisorption at 250°C followed by CO_2 desorption by N_2 purge at 350°C

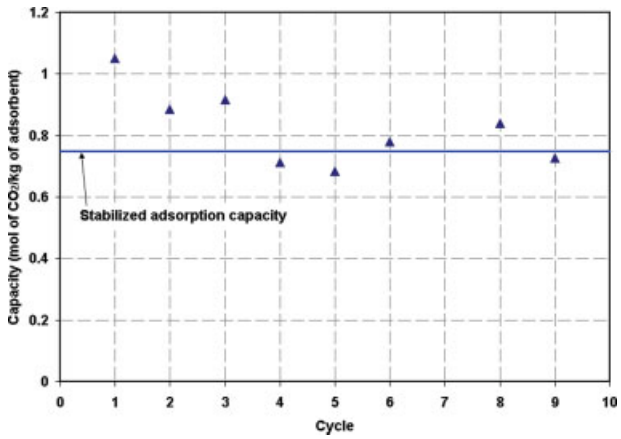

Figure 8. Example of cyclic stability of Na_2O promoted alumina.

[Color figure can be viewed in the online issue, which is available at www.interscience.wiley.com.]

indicate that a stable CO_2 sorption capacity can be achieved after a few cycles of operation.

Acknowledgments

The work was partly supported by the Pennsylvania Infrastructure Technology Alliance grants (PITA-442-04 and PITA-542-5), by the U.S. Department of Energy under cooperative agreement DE-PS26-04NT-42454, and by a donation from Air Products and Chemicals, Inc. The authors are grateful to Mr. J. McMullen and Ms. J. Purcell for construction of the test apparatus.

Literature Cited

1. Hufton JR, Mayorga S, Sircar S. Sorption-enhanced reaction process for hydrogen production. *AIChE J*. 1999;45:248−256.
2. Gaffney TR, Golden TC, Mayorga SG, Brzozowski JR, Taylor FW. Carbon dioxide pressure swing adsorption process using modified alumina adsorbents. U.S. Patent No. 5,917,136 (1999).
3. Hufton JR, Weigel SJ, Waldron WF, Rao MB, Nataraj S, Sircar S, Gaffney TR. Sorption enhanced reaction process for production of hydrogen. DOE-Air Products cooperative agreement. Instrument # DE-FC36–95G010059. Final Report 2000.
4. Ebner AD, Reynolds SP, Ritter JA. Understanding the adsorption and desorption behavior of CO_2 on a K-promoted hydrotalcite-like compound (HTlc) through nonequilibrium dynamic isotherms. *Ind Eng Chem Res*. 2006;45:6387−6392.
5. Ebner AD, Reynolds SP, Ritter JA. Nonequilibrium kinetic model that describes the reversible adsorption and desorption behavior of CO_2 in a K-promoted hydrotalcite-like compound. *Ind Eng Chem Res*. 2007;46:1737–1744.
6. Sircar S, Golden CMA. PSA process for removal of bulk carbon dioxide from a wet high temperature gas. U.S. Patent No. 6,322,612 (2001).
7. Ochoa-Fernandez E, Rusten HK, Jakobsen HA, Rønning M, Holmen A, Chen D. Sorption enhanced hydrogen production by steam methane reforming using Li_2ZrO_3 as sorbent: sorption kinetics and reactor simulation. *Catal Today*. 2005;106:41–46.
8. Waldron WE, Hufton JR, Sircar S. Production of hydrogen by cyclic sorption enhanced reaction process. *AIChE J*. 2001;47:1477–1479.
9. Sircar S, Hufton JR, Nataraj S. Sorption enhanced reaction process for hydrogen production. U.S. Patent No. 6,103,143 (2000).
10. Xiu GH, Li P, Rodrigues AE. Sorption-enhanced reaction process with reactive regeneration. *Chem Eng Sci*. 2002;57:3893–3908.
11. Xiu GH, Li P, Rodrigues AE. New generalized strategy for improving sorption-enhanced reaction process. *Chem Eng Sci*. 2003;58:3425–3437.
12. Wang YN, Rodrigues AE. Hydrogen production from steam methane reforming coupled with in situ CO_2 capture: conceptual parametric study. *Fuel*. 2005;84:1778–1789.
13. Lee KB, Beaver MG, Caram HS, Sircar S. Novel thermal swing sorption enhanced reaction process concept for hydrogen production by low-temperature steam-methane reforming. *Ind Eng Chem Res*. 2007;46:5003–5014.
14. Lee KB, Beaver MG, Caram HS, Sircar S. Production of fuel cell-grade hydrogen by thermal swing sorption enhanced reaction concept. *Int J Hydrogen Energy*. In press.
15. Lee KB, Beaver MG, Caram HS, Sircar S. Reversible chemisorption of carbon dioxide: simultaneous production of fuel-cell grade H_2 and compressed CO_2 from synthesis gas. *Adsorption*. In press.
16. Ding Y, Alpay E. Equilibria and kinetics of CO_2 adsorption on hydrotalcite adsorbent. *Chem Eng Sci*. 2000;55:3461–3474.
17. Yong Z, Rodrigues AE. Hydrotalcite-like compounds as adsorbents for carbon dioxide. *Energ Convers Mgmt*. 2002;43:1865–1876.
18. Yang JI, Kim JN. Hydrotalcite for adsorption of CO_2 at high temperature. *Kor J Chem Eng*. 2006;23:77–80.
19. Lee KB, Verdooren A, Caram HS, Sircar S. Chemisorption of carbon dioxide on potassium carbonate promoted hydrotalcite. *J Colloid Interf Sci*. 2007;308:30–39.
20. Sircar S, Golden TC. Isothermal and isobaric desorption of carbon dioxide by purge. *Ind Eng Chem Res*. 1995;34:2881–2888.
21. Young DM, Crowell AD. *Physical Adsorption of Gases*. Washington, DC: Butterworths, 1962.
22. Collins JJ. The LUB/equilibrium section concept for fixed-bed adsorption. *Chem Eng Prog Symp Ser*. 1967;63:31–35.
23. Levenspiel O. *Chemical Reaction Engineering: An Introduction to the Design of Reactors*. New York: John Wiley, 1962.
24. Sircar S, Hufton JR. Why does the linear driving force model for adsorption kinetics work? *Adsorption*. 2000;6:137–147.
25. Sircar S, Kumar R, Anselmo KJ. Effects of column nonisothermality or nonadiabaticity on the adsorption breakthrough curves. *Ind Eng Chem Proc Des Dev*. 1983;22:10–15.

Manuscript received Dec. 22, 2006, and revision received Aug. 3, 2007.